IOCFB 2024 Conference

The 1st International Online Conference on Functional Biomaterials

10–12 July 2024 | Online

Investigation of the corrosion mechanism of bifunctional FeMnSi-based alloys for medical applications

Ana-Maria Roman, Mihai-Adrian Bernevig, Gheorghe Bădărău, Ramona Cimpoeșu, Leandru-Gheorghe Bujoreanu, Nicanor Cimpoeșu*

Faculty of Materials Science and Engineering, ”Gheorghe Asachi” Technical University of Iasi, 41 D. Mangeron Blvd., 700050, Iasi, Romania

ana-maria.roman@academic.tuiasi.ro; nicanor.cimpoesu@academic.tuiasi.ro

INTRODUCTION & AIM

In the past few decades, researchers have investigated Fe-based biodegradable alloys for various purposes such as biocompatibility, tissue healing control over degradation rate, and the shape memory effect (SME) for specific medical applications. The study of pure Fe as a biodegradable alloy has brought to light a very low DR compared to Mg and Zn, which requires improvements to reach a compromise between the healing period and the maintenance of mechanical integrity for support.

In this study, the authors proposed Fe-Mn-Si based bifunctional alloys with Ag and Cu additions as potential biodegradable materials with SMEs for implantable medical applications. Isothermal dynamic strain scans were performed and their influence on corrosion resistance investigated. Macro and nano investigations of the corrosion compounds formed after immersion in Ringer's solution and SBF were conducted.

RESULTS & DISCUSSION

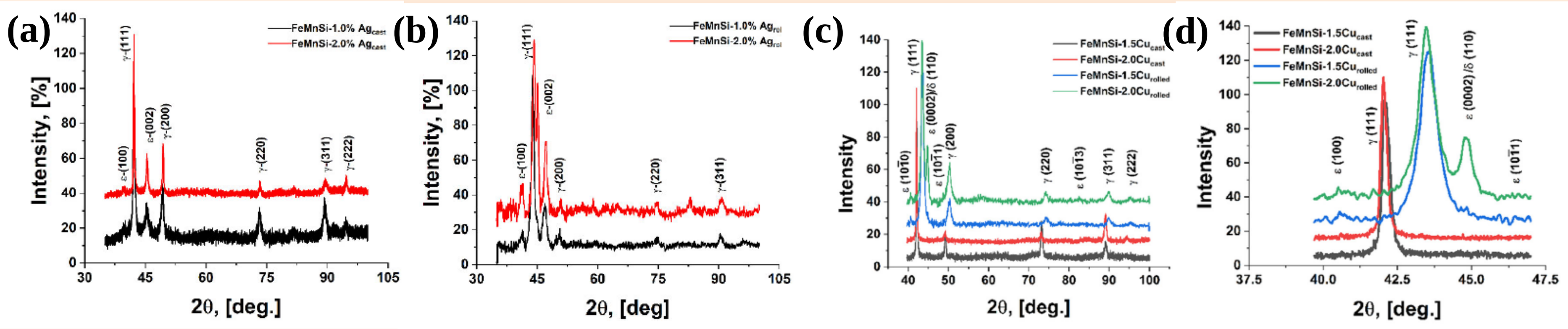

Figure 3. XRD spectra of the alloys: (a) cast FeMnSi-(1-2)Ag; (b) hot-rolled FeMnSi-(1-2)Ag; (c) FeMnSi-1.5Cu and FeMnSi-2Cu; (d) detail 40–47 (2θ).

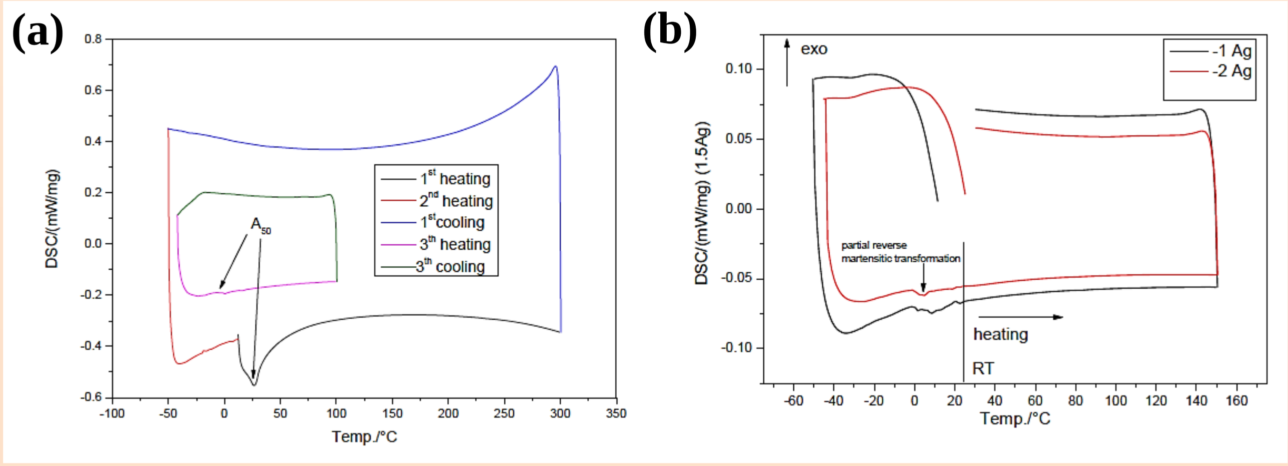

Figure 4. DSC diagrams for the hot rolled samples: FeMnSi-1Ag and FeMnSi-2Ag: (a) FeMnSi-2Ag for two heating/cooling cycles and (b) cooling - heating cycles of FeMnSi-1Ag and FeMnSi-2Ag.

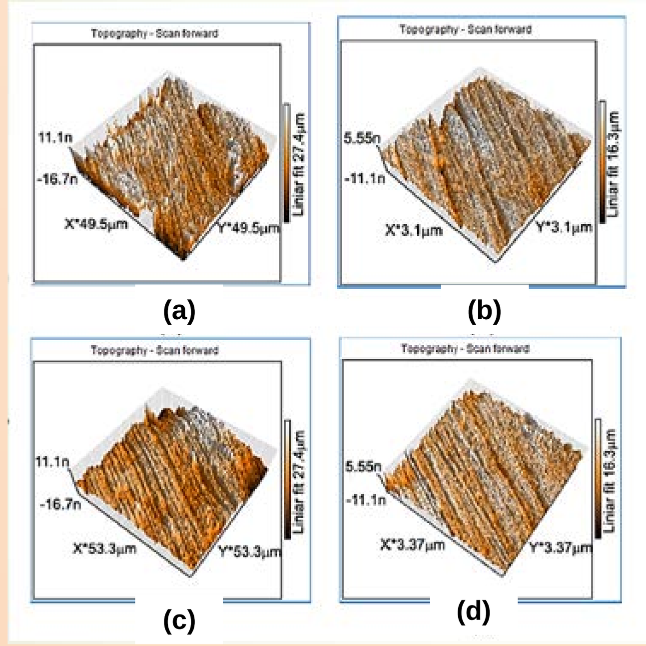

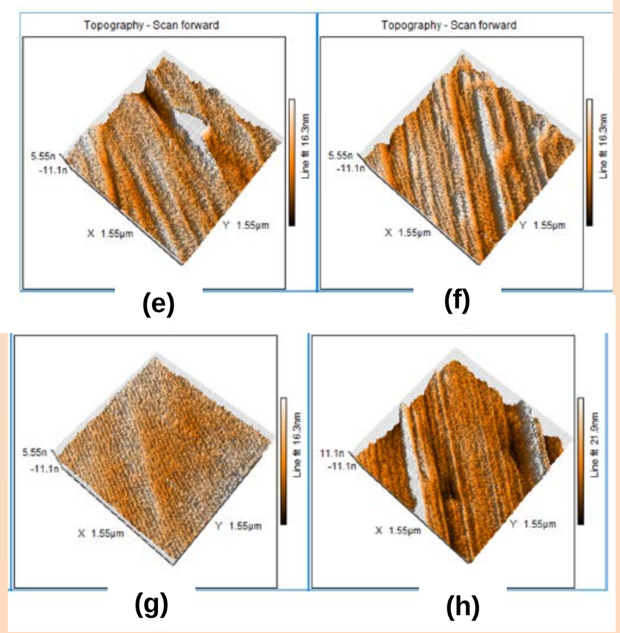

Figure 5. AFM images (3D topography) of the hot rolled plates before DMA_SS (1Hz): (a) FeMnSi–1Ag; (b) FeMnSi-2Ag; (e) FeMnSi-1.5Cu; (f)FeMnSi-2Cu; and after: (c) FeMnSi–1Ag; (d) FeMnSi-2Ag; (g) FeMnSi-1.5Cu; (h) FeMnSi-2Cu.

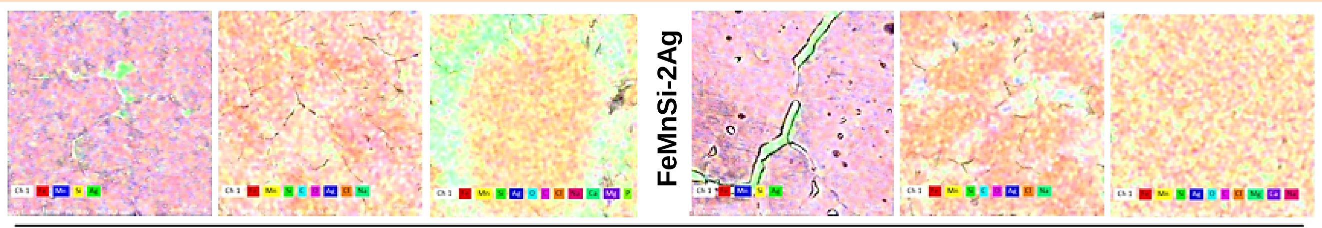

Chemical Elements/Sample	Fe Wt %	Fe At %	Mn Wt %	Mn At %	Si Wt %	Si At %	Ag Wt %	Ag At %	O Wt %	O At %	C Wt %	C At %	Na Wt %	Na At %	Cl Wt %	Cl At %	Ca Wt %	Ca At %
FeMnSi–1Ag	36.76	16.5	9.35	4.27	9.16	8.18	2.17	0.5	34.67	54.32	7.69	16.04	0.12	0.13	0.09	0.06	-	-
FeMnSi–2Ag	42.92	21.6	16.06	8.22	5.56	5.56	0.61	0.16	26.43	46.43	7.2	16.86	0.46	0.56	0.76	0.6	-	-
FeMnSi–1Ag (1 Hz)	42.34	20.54	14.63	7.21	4.05	3.9	0.57	0.14	30.7	51.97	6.88	15.52	0.14	0.16	0.6	0.46	0.02	0.01
FeMnSi–2Ag(1 Hz)	40.6	19.8	14.83	7.35	3.94	3.82	1.68	0.42	32.58	55.45	5.38	12.19	0.40	0.48	0.42	0.32	0.05	0.03
FeMnSi–2Ag(5 Hz)	44.97	24.02	19.17	10.41	5.62	5.97	0.36	0.1	21.02	39.19	7.6	18.87	0.83	1.08	0.21	0.18	-	-
FeMnSi–2Ag (20 Hz)	43.35	22.1	15.75	8.16	5.86	5.95	0.89	0.24	26.96	47.98	6.21	14.72	0.09	0.12	0.63	0.51	0.1	0.1
EDS err. %	0.9		0.1		0.1		0.05		1.9		0.7		0.2		0.2		0.1	

StDev: Fe: ±0.9, Mn: ±0.7, Si: ±0.22, Ag: ±0.4, O: ±0.2, C: ±0.1, Na: ±0.1, Cl: ±0.1, Ca: ±0.1.

Figure 6. EDS results after 14 days immersion in Ringer's solution – FeMnSi-(1-2)Ag hot rolled samples (initial, without DMA, and after DMA_SS.

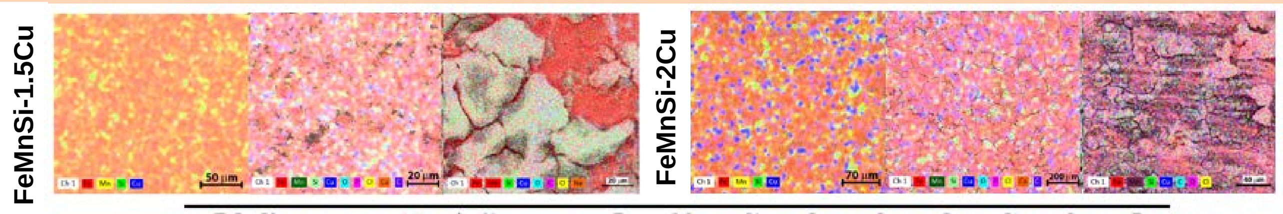

D I + U	Alloys/wt%		Fe	Mn	Si	Cu	O	C	Cl	Ca	P
1	FeMnSi-1.5Cu	C	70.7	2.36	4.99	1.53	9.66	10.2	-	-	0.38
		HR	49.8	25.1	4.32	1.52	11.8	5.9	-	0.29	1.27
	FeMnSi-2Cu	C	62.2	15.8	4.11	1.13	10.4	5.23	-	-	0.99
		HR	52.9	24.6	3.73	1.66	9.75	6.44	0.1	-	0.72
7	FeMnSi-1.5Cu	C	31.4	7.8	2.06	2.18	37.5	9.95	0.63	1.64	6.84
		HR	32.1	8.65	0.72	0.49	36.5	8.77	3.48	2.09	7.21
	FeMnSi-2Cu	C	34.3	4.18	1.41	0.13	37.6	11.8	0.8	1.44	8.34
		HR	28.9	7.73	0.41	0.25	40.9	7.93	1.81	2.5	9.54
14	FeMnSi-1.5Cu	C	29.6	13.6	6.03	5.79	34.6	9.44	0.38	-	-
		HR	29.1	14.2	3.74	5.74	37.1	9.73	0.21	-	-
	FeMnSi-2Cu	C	25.6	11.8	3.9	8.8	37.6	10.9	0.46		0.6
		HR	30.9	14.7	3.5	8.59	31.7	9.59	0.87	-	-
EDS detector error %			0.38	0.18	0.07	0.07	2.14	0.77	0.05	0.05	0.19

St.dev.: Fe: ±0.5; Mn: ±0.35; Si: ±0.2; Cu: ±0.2; O: ±1; C: ±0.25; Cl: ±0.1; Ca: ±0.01; P: ±0.01.

Figure 7. EDS results after 1,7,14 days immersion in SBF – FeMnSi-(1.5-2)Cu hot rolled and cast samples

METHODS

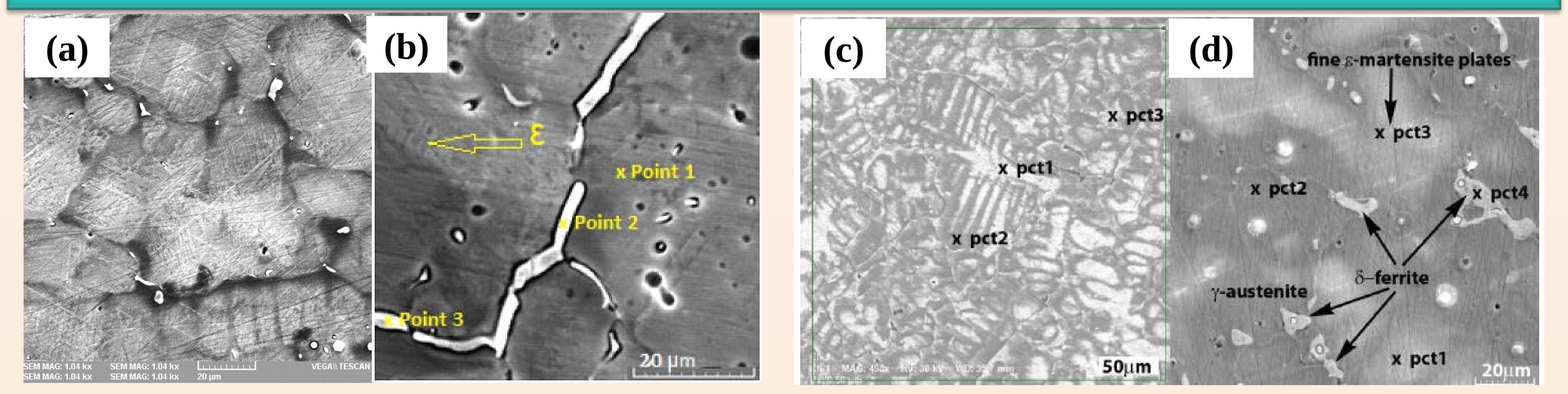

Figure 1. SEM images of alloys (produced in a cold crucible magnetic levitation induction furnace by melting and remelting the first ingots): (a) FeMnSi-1Ag; (b) FeMnSi-2Ag; (c) FeMnSi-1.5Cu; (d) FeMnSi-2Cu.

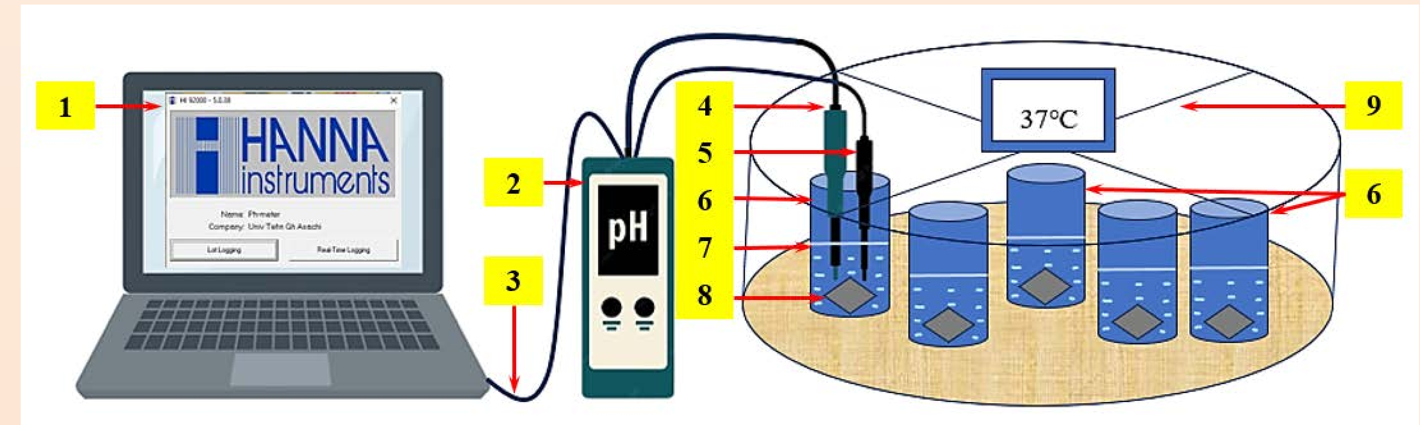

Ringer's: FeMnSi-1Ag, FeMnSi-2Ag – 3, 14 days

SBF: FeMnSi-1.5Cu, FeMnSi-2Cu – 1, 7, 14 days.

Figure 2. Installation scheme used for immersion tests (in SBF / Ringer's solution) and pH monitoring: 1- Hanna HI-92000 software; 2- Hanna HI98191 pH meter; 3- USB cable; 4- HI72911B titanium body pH electrode; 5- temperature sensor; 6- sample immersion container; 7- immersion solution; 8- sample; 9- constant-temperature climate control enclosure of 37 ℃.

CORROSION TESTS RESULTS

Samples (14 days immersion)	Without DMA_SS FeMnSi-1Ag	Without DMA_SS FeMnSi-2Ag	With DMA-SS FeMnSi-1Ag (1Hz)	With DMA-SS FeMnSi-2Ag(1Hz)	With DMA-SS FeMnSi-2Ag(5Hz)	With DMA-SS FeMnSi-2Ag(20Hz)
Initial mass (mg)	882.5	826.4	692.9	644.7	711.7	748.1
Mass after immersion (mg)	876.7 (-5.8)	843.1 (+16,7)	699.4 (+6.5)	646.2 (+1.5)	708 (-3.7)	760.3 (+12.2)
Mass after ultrasound (mg)	876 (-6.5)	818.5 (-7.9)	686.8 (-6.1)	636.3 (-8.4)	704.2 (-7.5)	737.7 (-10.4)
Corrosion rate (μm/y)	**64**	**79**	**82**	**113**	**101**	**140**

The samples areas without DMA-SS: FeMnSi-1Ag = 3.3 cm² and FeMnSi-2Ag= 3.1 cm²; with DMA-SS: FeMnSi-1Ag, FeMnSi-2Ag(I), FeMnSi-2Ag(II), FeMnSi-2Ag(III) =2.6 cm².

FeMnSi-1.5Cu	1 day C	1 day HR	7 days C	7 days HR	14 days C	14 days HR
Initial mass (mg)	6007.4	698.2	3192.4	851	3471.6	794
Mass after immersion (mg)	6010.2 (+2.8)	697.4 (-0.8)	3153.8 (-38.6)	858.6 (+7.6)	3436.8 (-34.8)	767.6 (-26.4)
Mass after ultrasound (mg)	6005.9 (-1.5)	697.3 (-0.9)	3147.2 (-45.2)	844.8 (-6.2)	3434.4 (-37.2)	766.9 (-27.1)
Corrosion rate (μm/y)	**108**	**184**	**536**	**145**	**200**	**327**

FeMnSi-2Cu	1 day C	1 day HR	7 days C	7 days HR	14 days C	14 days HR
Initial mass (mg)	5628.8	716.8	4886.4	977.1	6122.4	1100.5
Mass after immersion (mg)	5629.9 (+1.1)	716.4 (-0.4)	4855.8 (-30.6)	970.3 (-6.8)	6063.8 (-58.6)	1102.7 (+2.2)
Mass after ultrasound (mg)	5628.6 (-0.2)	716.2 (-0.6)	4850 (-36.4)	966.6 (-10.5)	6058 (-64.4)	1087 (-13.5)
Corrosion rate (μm/y)	**16**	**134**	**418**	**204**	**369**	**115**

The sample areas: 1.5Cu (1 day) C= 6.8 cm², 1.5Cu (1 day) HR=2.4 cm², 1.5Cu (7 days) C =5.9 cm², 1.5Cu (7 days) HR =3 cm², 1.5Cu (14 days) C =6.5 cm², 1.5Cu (14 days) HR =2.9 cm²; 2%Cu (1 day) C= 6.1 cm², 2Cu (1 day) HR=2.2 cm², 2Cu (7 days) C =6.1 cm², 2Cu (7 days) HR =3.6 cm², 2Cu (14 days) cast =6.1 cm², 2Cu (14 days) HR =4.1 cm².

Figure 8. Corrosion rates determined after immersion in Ringer's solution - FeMnSi-(1-2)Ag and SBF – FeMnSi-(1.5-2)Cu (gravimetric method).

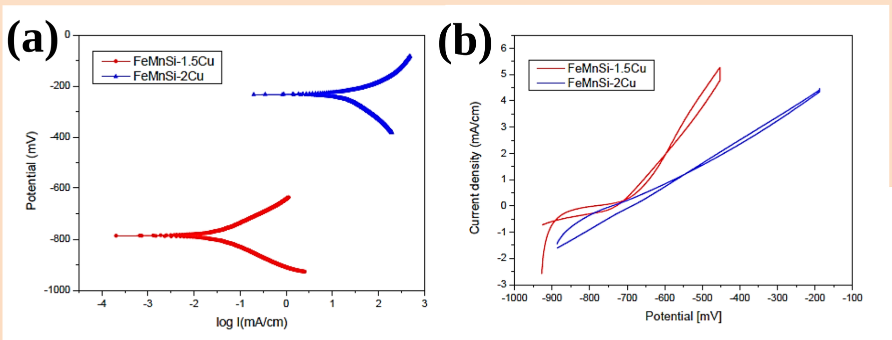

Figure 9. Electrochemical Corrosion Resistance Tests (a) Tafel, (b) cyclic potentiometry, (c) parameters.

(c)

Sample	E_0 mV	b_a mV	b_c mV	R_p ohm·cm²	J_{corr} mA/cm²	V_{corr} μm/Year
FeMnSi-1.5Cu	–786	92	–85	638	32.1	374
FeMnSi-2Cu	–232	68	–124	847	17.37	203

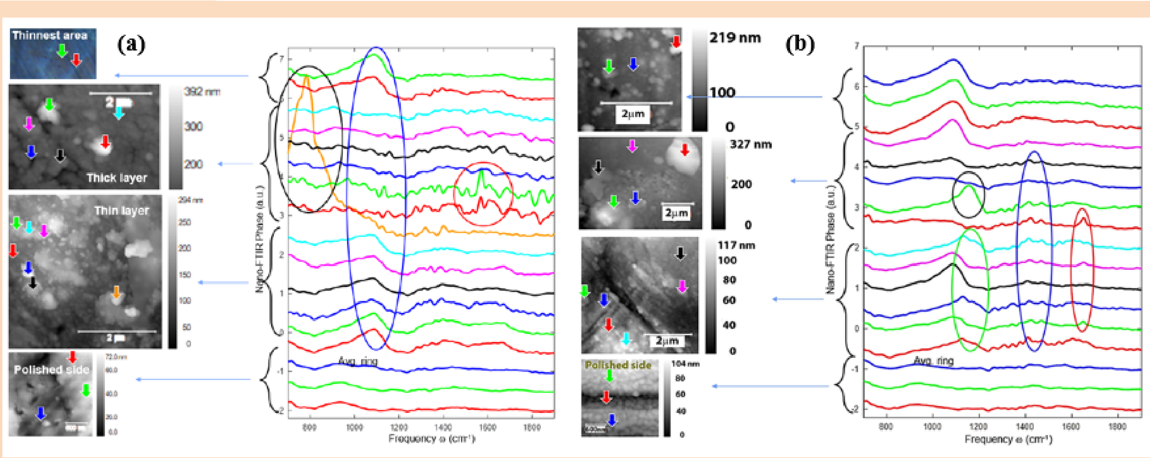

Figure 10. Nano-FTIR analysis results. Scanned surface and the dedicated FTIR spectra of the particles observed on the alloys: (a) FeMnSi-2Ag; (b) FeMnSi-2Cu.

CONCLUSION AND FUTURE WORK

DSC results validate medical usability of FeMnSi-based functional material with an A_{50} temperature. With a specific thermo-mechanical treatment to modify the transformation temperatures, an intelligent Fe-based biodegradable alloy can be used in the medical field. Future research is aimed in developing a complex mathematical model of the whole degradation process based on experimental results, mathematical hypotheses and computer simulations.

REFERENCES:

[1] Gasior, G.; Szczepanski, J.; Radtke, A., *Materials* **2021**, 14, 3381.

[2] Gorejová, R.; Haverová, L.; Orinaková, R.; Orinak, A.; Orinak, M., *J. Mater. Sci.* **2019**, 54, 1913–1914.

[3] Roman, A.M.; Cimpoes,u, R.; Pricop, B.; Lohan, N.M.; Cazacu, M.M.; Bujoreanu, L.G.; Panaghie, C.; Zegan, G.; Cimpoesu, N.; Murariu, A.M., *J. Funct.Biomater.* **2023**, 14, 377.

[4] Roman, A.-M.; Cimpoeșu, R.; Pricop, B.; Cazacu, M.M.; Zegan, G.; Istrate, B.; Cocean, A.; Chelariu, R.; Moscu, M.; Bădărău, G.; Cimpoesu, N.; Ivănescu, M.C., *Nanomaterials* **2024**, 14, 330.

Acknowledgments: Special thanks to Iban Amenabar from CIC NanoGUNE BRTA for conducting the experiments on the nano-FTIR (nea-Spec) equipment and Adrian Cernescu from Attocube Neaspec for his support and excellent collaboration.

Electron Microscopy and Chemical Analysis Laboratory: https://esimsim.ro/